Article

Protecting the global ocean for biodiversity, food and climate

https://doi.org/10.1038/s41586-021-03371-z

Received: 19 December 2019

Accepted: 18 February 2021

Check for updates

Enric Sala[1]✉, Juan Mayorga[1,2], Darcy Bradley[2], Reniel B. Cabral[2], Trisha B. Atwood[3], Arnaud Auber[4], William Cheung[5], Christopher Costello[2], Francesco Ferretti[6], Alan M. Friedlander[1,7], Steven D. Gaines[2], Cristina Garilao[8], Whitney Goodell[1,7], Benjamin S. Halpern[9], Audra Hinson[3], Kristin Kaschner[8], Kathleen Kesner-Reyes[10], Fabien Leprieur[11], Jennifer McGowan[12], Lance E. Morgan[13], David Mouillot[11], Juliano Palacios-Abrantes[5], Hugh P. Possingham[14], Kristin D. Rechberger[15], Boris Worm[16] & Jane Lubchenco[17]

The ocean contains unique biodiversity, provides valuable food resources and is a major sink for anthropogenic carbon. Marine protected areas (MPAs) are an effective tool for restoring ocean biodiversity and ecosystem services[1,2], but at present only 2.7% of the ocean is highly protected[3]. This low level of ocean protection is due largely to conflicts with fisheries and other extractive uses. To address this issue, here we developed a conservation planning framework to prioritize highly protected MPAs in places that would result in multiple benefits today and in the future. We find that a substantial increase in ocean protection could have triple benefits, by protecting biodiversity, boosting the yield of fisheries and securing marine carbon stocks that are at risk from human activities. Our results show that most coastal nations contain priority areas that can contribute substantially to achieving these three objectives of biodiversity protection, food provision and carbon storage. A globally coordinated effort could be nearly twice as efficient as uncoordinated, national-level conservation planning. Our flexible prioritization framework could help to inform both national marine spatial plans[4] and global targets for marine conservation, food security and climate action.

The global ocean is a trove of biodiversity, containing unique life forms and genetic resources that provide ecosystem services of enormous value to humans[2,5]. However, increasing anthropogenic effects are compromising the ability of the ocean to provide these services[6,7] and have motivated a global discussion about expanding the world's system of MPAs.

MPAs—especially highly protected areas in which extractive and destructive activities are banned[8,9]—can be effective management tools to safeguard and restore ocean biodiversity and associated services[1,2,10], complement conventional fisheries management and contribute to the mitigation of climate change by protecting marine carbon stocks[11]. Yet as of March 2021, only around 7% of ocean area has been designated or proposed as MPAs, and only 2.7% is actually implemented as fully or highly protected[3]. This low level of ocean protection is explained in part by conflict between protection and extraction stemming from perceived trade-offs. Rather than viewing protection versus extraction as a zero-sum game, we ask whether strategic conservation planning can simultaneously yield benefits for biodiversity conservation, food provisioning and carbon storage.

Previous efforts to identify global conservation priorities in the ocean have primarily focused on narrow definitions of biodiversity and ignored other key facets such as functional roles, evolutionary histories of species and unique community assemblages[12,13]. Perhaps more importantly, focusing on a single objective in a multi-use ocean often results in strong trade-offs that hinder real-world conservation action. To overcome these problems, we developed a comprehensive conservation planning framework to achieve multiple objectives: biodiversity protection, food provisioning and carbon storage. The framework considers human impacts that are abatable through highly or fully protected MPAs (that is, protection from fishing, mining and habitat destruction) and those that are un-abatable with those tools[14] (for example, nutrient pollution, ocean warming and acidification), and it seeks to maximize the difference made by protection relative to a business-as-usual scenario (that is, a world without additional

[1]Pristine Seas, National Geographic Society, Washington, DC, USA. [2]Environmental Market Solutions Lab, University of California Santa Barbara, Santa Barbara, CA, USA. [3]Department of Watershed Sciences and Ecology Center, Utah State University, Logan, UT, USA. [4]IFREMER, Unité Halieutique de Manche et Mer du Nord, Boulogne-sur-Mer, France. [5]Changing Ocean Research Unit, Institute for the Oceans and Fisheries, The University of British Columbia, Vancouver, British Columbia, Canada. [6]Department of Fish and Wildlife Conservation, Virginia Polytechnic Institute and State University, Blacksburg, VA, USA. [7]Hawai'i Institute of Marine Biology, Kāne'ohe, HI, USA. [8]Evolutionary Biology and Ecology Laboratory, Albert Ludwigs University, Freiburg, Germany. [9]National Center for Ecological Analysis and Synthesis (NCEAS), University of California, Santa Barbara, CA, USA. [10]Quantitative Aquatics, Los Baños, The Philippines. [11]MARBEC, Université de Montpellier, Montpellier, France. [12]The Nature Conservancy, Arlington, VA, USA. [13]Marine Conservation Institute, Seattle, WA, USA. [14]Centre for Biodiversity and Conservation Science (CBCS), The University of Queensland, Brisbane, Queensland, Australia. [15]Dynamic Planet, Washington, DC, USA. [16]Ocean Frontiers Institute, Dalhousie University, Halifax, Nova Scotia, Canada. [17]Oregon State University, Corvallis, OR, USA. ✉e-mail: esala@ngs.org

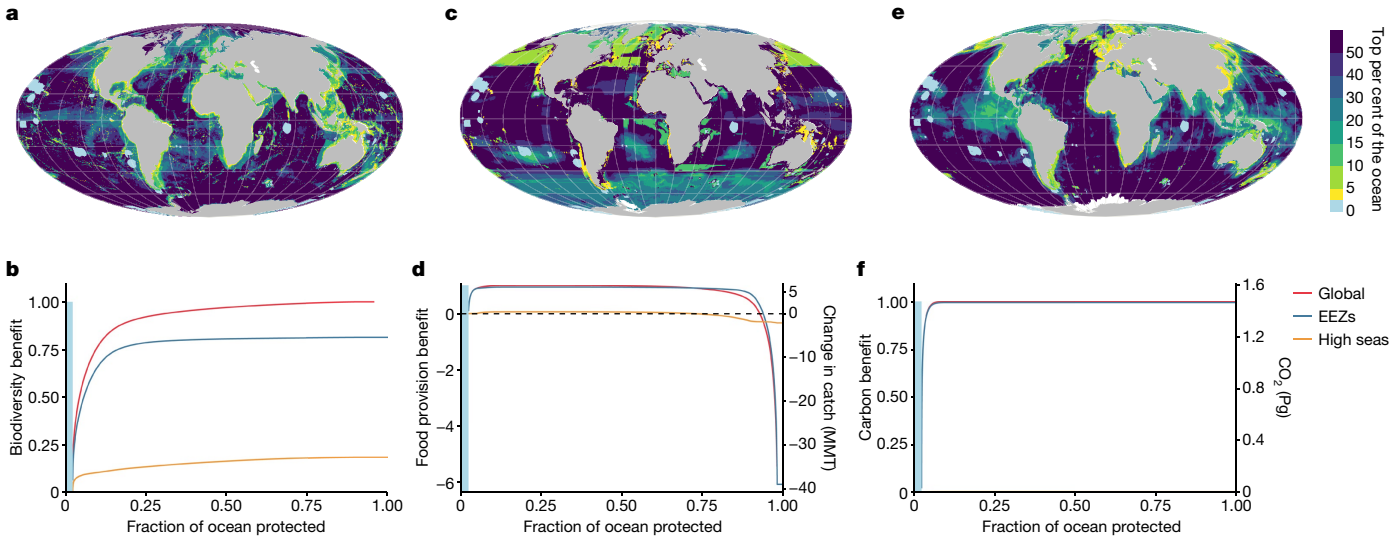

Fig. 1 | Global conservation priorities. a, **c**, **e**, Prioritization of a global network of MPAs for biodiversity conservation (**a**), food provisioning (**c**) and carbon stocks (**e**). Existing fully protected areas are shown in light blue. **b**, **d**, **f**, Corresponding cumulative benefit functions, in which 'benefits' are defined as conservation gains (for biodiversity) (**b**), net change in the catchable species of fisheries owing to spillover from marine protected areas (for food provisioning) (**d**) and reduction of the risk of carbon disturbance due to bottom trawling (for carbon) (**f**). Cumulative global benefits and those accruing from protection of the high seas and EEZs are shown separately. The blue bar in the benefit curves denotes the current 2.7% of the global ocean that is included in fully protected areas.

protection). Furthermore, it does not require area-based targets set a priori, but instead produces a hierarchy of marine conservation priorities across scales.

Biodiversity conservation

Marine biodiversity is the variety of life in the sea, encompassing variation at many levels of complexity, from within taxa to ecosystems. Thus, we sought to identify areas where MPAs would be most effective at achieving multiple biodiversity conservation goals, including minimizing species extinction risk, maintaining diverse species traits in ecosystems, and preserving the evolutionary history of marine life, while ensuring biogeographical representation. To this end, we define the biodiversity benefit of a given network of MPAs as the weighted sum of the marginal gain in persistence of specific biodiversity features resulting from the removal of abatable impacts relative to business as usual[15] (see Methods).

Our results show that priority areas for biodiversity conservation are distributed throughout the ocean, with 90% of the top 10% priority areas contained within the 200-mile exclusive economic zones (EEZs) administered by individual coastal nations (Fig. 1a). These EEZs are home to irreplaceable biodiversity and are often heavily affected by human activities that can be abated by MPAs[16] (Supplementary Fig. 1). However, we also find many priority areas in the high seas around seamount clusters, offshore plateaus and biogeographically unique areas such as the Antarctic Peninsula, the Mid-Atlantic Ridge, the Mascarene Plateau, the Nazca Ridge and the Southwest Indian Ridge (Supplementary Fig. 2).

Global biodiversity benefits accrue rapidly with protection of the highest priority areas (Fig. 1b). We find that we could achieve 90% of the maximum potential biodiversity benefits from MPAs by strategically protecting 21% of the ocean (43% of EEZs and 6% of the high seas). This would markedly increase the average protection of endangered and critically endangered species from currently 1.5% and 1.1% of their ranges to 82% and 87%, respectively, and would increase the average protection of biogeographical provinces by a factor of 24 (Supplementary Figs. 3, 4).

Climate change is already modifying the distributions of marine species and is expected to continue to do so[17]. Hence the biodiversity benefits of any MPA network that is designed for current conditions may change in the future[18]. To assess these putative changes, we re-assess our biodiversity prioritization using projected species distributions for 2050 under a 'high greenhouse gas emissions' scenario (Intergovernmental Panel on Climate Change (IPCC) Special Report on Emissions Scenarios (SRES) A2[19–21]; see Methods). We find that around 80% of areas that are within the top 10% global biodiversity priorities today will remain so in 2050 (Supplementary Fig. 5). Some temperate regions and parts of the Arctic would rank as higher priorities for biodiversity conservation by 2050, whereas large areas in the high seas between the tropics and areas in the Southern Hemisphere would decrease in priority.

Food provisioning

In highly and fully protected MPAs, the biomass of commercially targeted fishes and invertebrates increases over time, and given the right biological conditions, may also enhance productivity in fished areas outside of the MPA through adult and larval spillover[22–24]. Where overfishing is occurring, MPAs can increase food provisioning; where fisheries are well-managed or exploited below the maximum sustainable yield (MSY), this effect can be muted or reversed[25,26]. Thus, we identify priority areas that would improve future yields of fisheries by modelling the effects of protection on 1,150 commercially exploited marine stocks (representing around 71% of global MSY[27]), accounting for their current management status, exploitation level, fishing effort redistribution and relevant biological attributes[28]. Because the redistribution of fishing effort after the implementation of MPAs can affect food provisioning outcomes, we model two different scenarios. The first assumes that displaced fishing effort from MPAs relocates to the remaining fished areas outside MPAs proportionally to previous effort allocation (see Methods). The second assumes no redistribution, such that fishing effort outside the MPA remains constant.

We find that, under the full effort displacement assumption, strategically placed MPAs that cover 28% of the ocean could increase

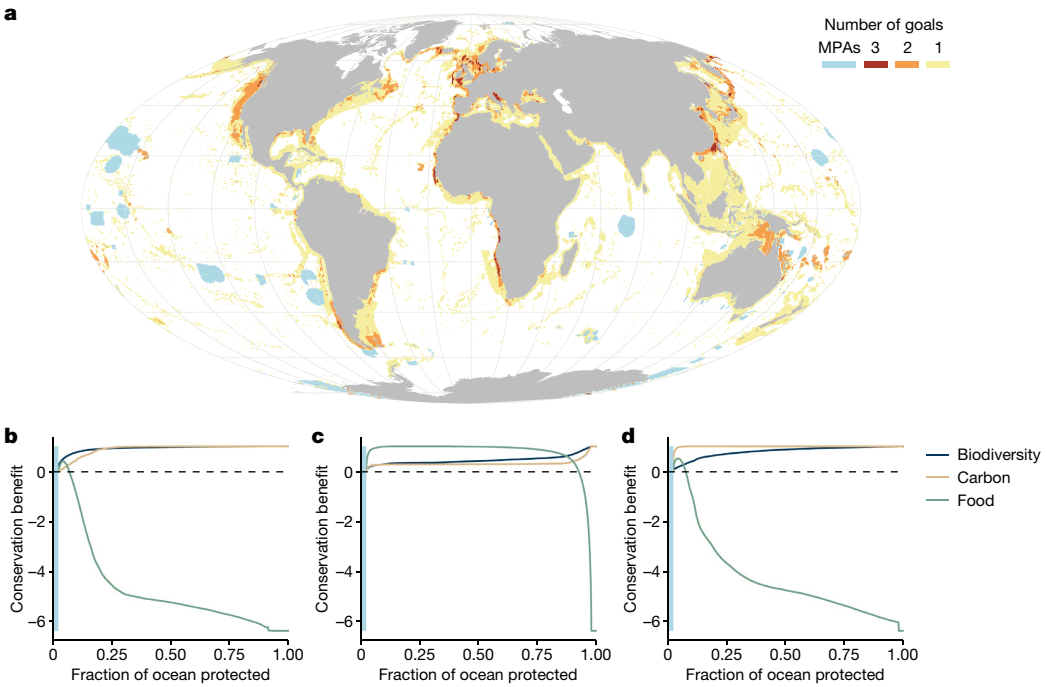

Fig. 2 | Co-benefits of protection. a, Priority areas to achieve 90% of the maximum benefits for one (yellow), two (orange) and three (red) simultaneous conservation objectives (biodiversity conservation, carbon stocks and food provisioning). Existing fully protected areas are shown in light blue. **b**–**d**, Cumulative co-benefits for each goal under a single-objective prioritization of biodiversity (**b**), food provisioning (**c**) and carbon (**d**). The blue bar in the benefit curves denotes the current 2.7% of the global ocean that is included in fully protected areas.

food provisioning by 5.9 million metric tonnes (MMT) relative to a business-as-usual scenario with no additional protection and unabated fishing pressure (Fig. 1d). Achieving 90% of this potential would require strategic protection of 5.3% of the ocean (Supplementary Fig. 6). This result reflects only data-rich stocks; a conservative scaled-up estimate including all stocks globally would produce a yield increase of 8.3 MMT (see Methods). Assuming that fishing effort outside MPAs remains constant, the maximum increase in yield decreases to 5.2 MMT (7.3 MMT when including all stocks), and the area needed to capture 90% of these benefits would decrease to 3.8% of the ocean (Supplementary Figs. 7, 8). Areas with the largest food provisioning potential were located within EEZs (Fig. 1c), which currently provide 96% of global catch and contain most of the world's overexploited fisheries[22]. The concomitant changes in catchable biomass will take time to accrue, and will vary across species and locations. Notably, if fishery management were to improve globally, the food provisioning case for MPAs would diminish.

Carbon storage

Marine sediments are the largest pool of organic carbon on the planet and a crucial reservoir for long-term storage[29]. If left undisturbed, organic carbon stored in marine sediments can remain there for millennia[30]. However, disturbance of these carbon stores can re-mineralize sedimentary carbon to CO_2, which is likely to increase ocean acidification, reduce the buffering capacity of the ocean and potentially add to the build-up of atmospheric CO_2. Thus, protecting the carbon-rich seabed is a potentially important nature-based solution to climate change[11,31].

Using satellite-inferred information on fishing activity by industrial trawlers and dredgers between 2016 and 2019, aggregated at a resolution of 1 km^2, we estimate that 4.9 million km^2 or 1.3% of the global ocean is trawled each year. This disturbance to the seafloor results in an estimated 1.47 Pg of aqueous CO_2 emissions, owing to increased carbon metabolism in the sediment in the first year after trawling. If trawling continues in subsequent years, emissions decline as sediment carbon stocks become exhausted. However, after 9 years of continuous trawling, emissions stabilize at around 40% of the first year's emissions, or around 0.58 Pg CO_2 (Supplementary Fig. 35). If the intensity and footprint of trawling remains constant, we estimate that sediment carbon emissions will continue at approximately 0.58 Pg CO_2 for up to around 400 years of trawling, after which all of the sediments in the top metre are depleted. Although 1.47 Pg CO_2 represents only 0.02% of total marine sedimentary carbon, it is equivalent to 15–20% of the atmospheric CO_2 absorbed by the ocean each year[32,33], and is comparable to estimates of carbon loss in terrestrial soils caused by farming[34]. Although an unknown fraction of the aqueous CO_2 is emitted to the atmosphere, the increase in CO_2 in the water column and sediment pore waters can have far-reaching and complex effects on marine carbon cycling, primary productivity and biodiversity[29,35].

We identify areas where MPAs can effectively prevent the remineralization of sediment carbon to CO_2 that results from anthropogenic disturbances[36]. Top priority areas are located where carbon stocks and present anthropogenic threats are highest, including China's EEZ, Europe's Atlantic coastal areas, and productive upwelling areas (Fig. 1e). Countries with the highest potential to contribute to the mitigation of climate change through protection of carbon stocks are those with large EEZs and large industrial bottom trawl fisheries. The global benefit of protection for sediment carbon accrues sharply, because the spatial footprint of bottom trawling is small. At our working resolution of 50 km × 50 km, eliminating 90% of the present risk of carbon disturbance due to bottom trawling would require protecting 3.6% of the ocean (mostly within EEZs) (Fig. 1f). Deep-sea mining is another emerging threat to sediment carbon, but its spatial footprint is so far unknown as this industry is only now developing.

Multi-objective prioritization

We conduct three separate analyses for multi-objective prioritization. First, we explore synergies across objectives by overlaying

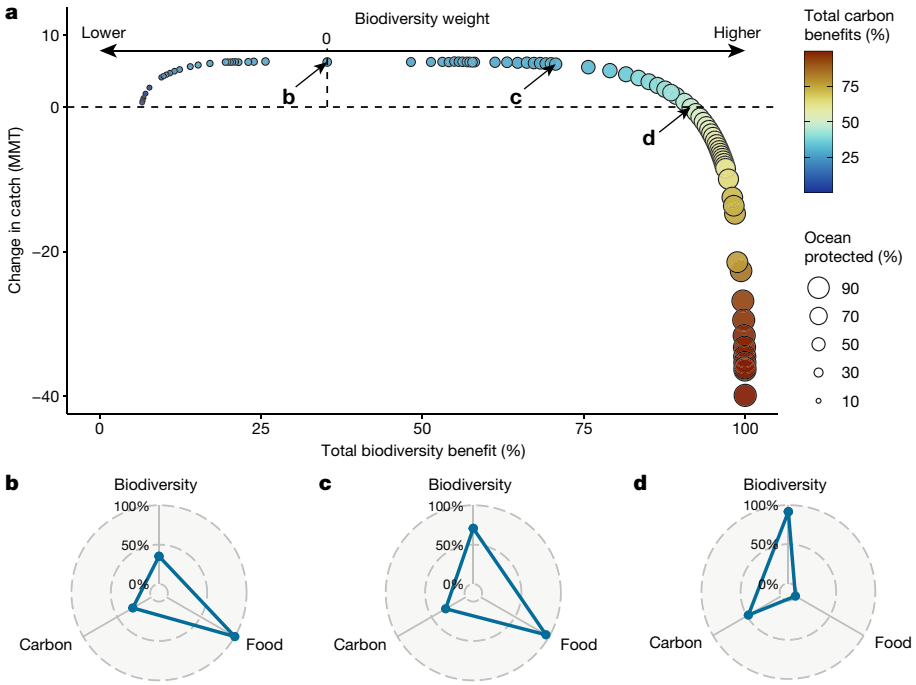

Fig. 3 | Prioritizing multiple objectives given unknown preferences. a, Each point represents the spatial configuration (Supplementary Figs. 10–12) that maximizes the net benefits of protection for an assigned weight (preference) to biodiversity in a joint biodiversity–food provisioning prioritization, under the assumption that fishing effort on a stock from an area designated for protection displaces to the area outside the MPA (see Supplementary Fig. 13 for an alternative scenario without redistribution of fishing effort). Carbon was treated as a co-benefit (weight = 0). Arrows and labels refer to the scenarios depicted in the bottom panels. **b**, Optimal conservation strategy if biodiversity is given a weight of zero. This scenario achieves 100% of the potential fisheries benefit by protecting the 28% top priority areas of the ocean, and achieves 35% of biodiversity benefits and 27% of carbon benefits. **c**, Optimal conservation strategy if biodiversity is given the same weight as food provisioning. This scenario protects 45% of the ocean, yielding 92% of the potential fisheries benefits, 71% of biodiversity benefits and 29% of carbon benefits. **d**, Optimal conservation strategy with strong biodiversity preference (14 × food provisioning weight). This scenario achieves 91% of the biodiversity benefit at the least cost to future fisheries yields and achieves 48% of the carbon benefit by protecting 71% of the global ocean.

single-objective priority maps to create a composite multi-objective solution[37]. Overlaying the areas required to achieve 90% of the benefit for each conservation objective, we find that unprotected triple-benefit areas are spread across the world's EEZs in all continents, covering 0.3% of the global ocean (Fig. 2a). Double-benefit areas (combinations of two out of three objectives) cover 2.7% of total ocean area.

Our second approach involves estimating the co-benefits that arise from single-objective prioritizations (Fig. 2b–d). For instance, we find that achieving 90% of the biodiversity benefit following the optimal single-objective prioritization would coincidently protect 89% of at-risk carbon stocks, but would come at a cost of 27 MMT of catchable fish. Although these two approaches are instructive, selecting sites for protection on the basis of overlapped benefits or co-benefits often results in strong trade-offs between objectives that could be reduced by a jointly optimized network of MPAs.

Our third and preferred approach is to conduct joint multi-objective optimization. This approach allows for stakeholder preferences to inform priorities, which are captured by assigning weights to each objective. As a decision-support framework, multi-objective prioritization is well-suited to assess multiple benefits given different scenarios or preferences.

To illustrate this approach, we derive an efficiency frontier for the biodiversity and food provision objectives (Fig. 3a) that maximizes net benefits across a range of possible preferences (expressed as objective weights). Although our framework can consider explicit preferences for each and any objective, we treat carbon as a co-benefit (weight = 0) to facilitate visualization and interpretation (see Supplementary Fig. 14 for a multi-objective prioritization with equal weights given to each of the three goals). If society were to value marine biodiversity benefits as much as food provision benefits (see Methods), the optimal conservation strategy would protect 45% of the ocean, delivering 71% of the maximum possible biodiversity benefits, 92% of food provisioning benefits and 29% of carbon benefits (Fig. 3c, Supplementary Fig. 10). Results also suggest that we could protect as much as 71% of the ocean, obtaining 91% of the biodiversity and 48% of the carbon benefits, with no change in the future yields of fisheries (Fig. 3d, Supplementary Fig. 11). If, on the contrary, we placed no value on biodiversity, the optimal strategy would call for the protection of 28% of the ocean, providing a net gain of 5.9 MMT of seafood (8.3 MMT when accounting for unassessed stocks) and incidentally securing 35% of biodiversity benefits and 27% of carbon benefits (Fig. 3b, Supplementary Fig. 12). Only if biodiversity is deemed undesirable (negative weight) would it be optimal to protect less than 28% of the ocean. Assuming no redistribution of fishing effort after protection, the analysis yields a slightly different efficiency curve. In this case, giving no value to biodiversity would call for protection of 12% of the ocean (Supplementary Figs. 10–13).

The need for international cooperation

Global-scale prioritization helps to focus attention and resources on places that yield the largest possible benefits. A particular advantage of our approach is the ability to quantify how international cooperation in the expansion of MPAs can facilitate greater benefits for all three of our objectives simultaneously. To demonstrate this, we calculated the cumulative biodiversity benefit of protecting areas from highest to lowest priority under three strategies: (1) systematic expansion of MPAs considering global priorities; (2) systematic expansion of MPAs within EEZs and the high seas considering only national priorities;

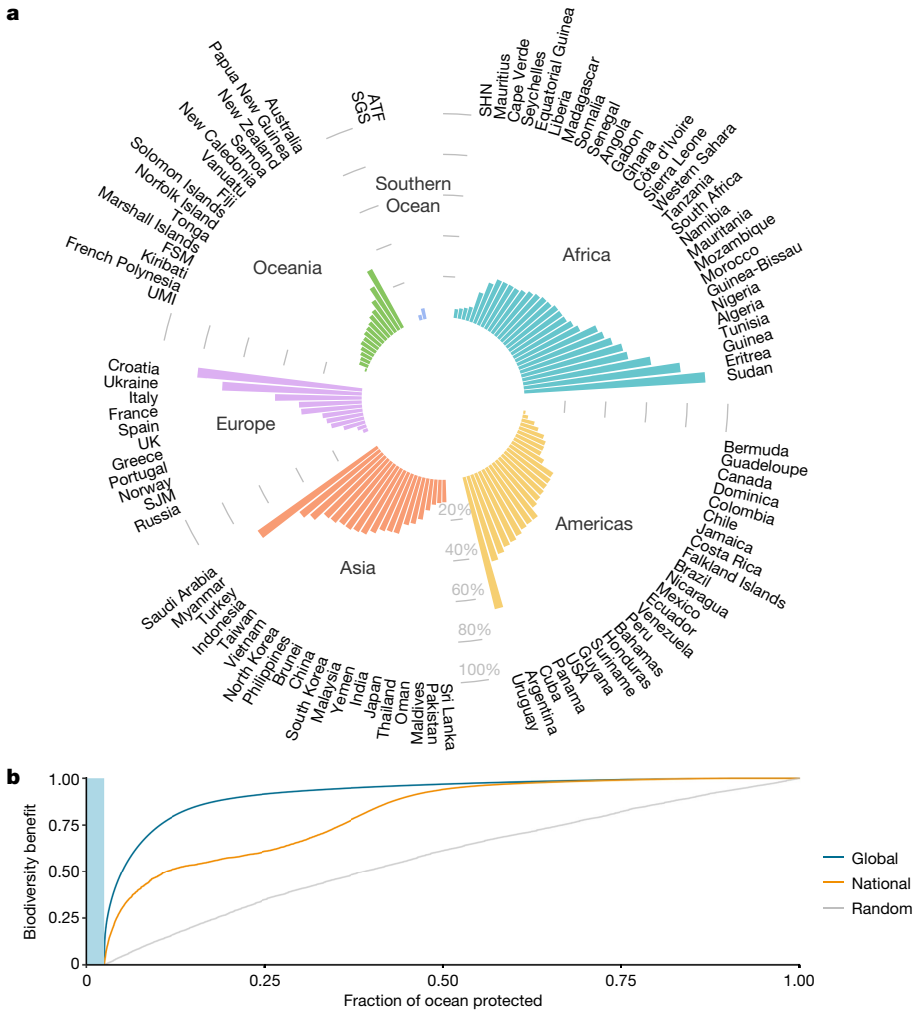

Fig. 4 | National contributions to biodiversity conservation and coordinated implementation. **a**, Fraction of nations' EEZs in the top 10% of priority areas for global marine biodiversity conservation. Shown here are the 100 countries or territories with the largest contributions towards achieving the maximum possible biodiversity benefit. Values are in addition to current protection. **b**, Cumulative biodiversity conservation benefit from implementing a globally coordinated MPA expansion according to global priorities (blue), national priorities (orange), and random placement (grey; 100 random sets). The blue bar denotes the current 2.7% of the global ocean that is included in fully protected areas. ATF, French Southern Territories; FSM, Federated States of Micronesia; SGS, South Georgia and the South Sandwich Islands; SHN, Saint Helena, Ascension and Tristan da Cunha; SJM, Svalbard and Jan Mayen; UMI, United States Minor Outlying Islands.

and (3) random allocation of MPAs (see Methods). We find that a globally coordinated effort could achieve 90% of the maximum possible biodiversity benefit with less than half the ocean area of a protection strategy that is based solely on national priorities (21% versus 44% of the ocean, respectively) (Fig. 4b). A comparable analysis of global priorities to expand the network of terrestrial protected areas similarly found large efficiency gains from global coordination[38]. A random approach to conservation is the least efficient and would require protection of 85% of the ocean to achieve the same results.

Discussion

There is a growing consensus that ocean conservation can deliver lasting benefits to biodiversity, climate mitigation and food security. Our framework shows that strategic conservation planning can reconcile seemingly conflicting objectives using strategic and efficient prioritization for MPAs at both global and national scales.

Our results highlight the need for a greater level of investment in MPAs than we have at present, regardless of the preferences of the stakeholders involved. We recognize that such change, along with the required improvements to enforcement and compliance, could be challenging to implement. One possible path forward is to upgrade the level of protection and management effectiveness of existing but weakly protected MPAs that are located in areas of the highest priority (Supplementary Fig. 15), so that they can deliver their full suite of benefits. We found that this cannot be achieved by a few countries alone; especially when considering co-benefits, there is an important role for most coastal countries to help to achieve each of the objectives considered in this analysis (Fig. 4a, Supplementary Figs. 16, 17). Concerns over potential inequities will need to be addressed through international cooperation, including sustainable financing mechanisms to reduce potential short-term burdens on nations with disproportionately large priority areas.

Food provisioning benefits also require improved fisheries management, which should go hand in hand with improved conservation efforts—for example, in addressing the potential problems that are associated with fishing effort redistribution. Here we do not promote MPAs as the best fisheries management tool, but rather show that MPAs can improve the yield of fisheries, while also protecting biodiversity, carbon stocks and other ecosystem services. MPAs and responsible fisheries management are not mutually exclusive; rather, they are complementary.

Our analysis makes a series of assumptions. First, we assume that the current distribution of human impacts is a good proxy to estimate 'no additional protection' counterfactuals. However, human impacts on the ocean are dynamic and will continue to change into the future. Nevertheless, current threats often have lasting effects that are captured well by our prioritization framework. As an alternative, we estimate a worst-case scenario in which we assume that everything that is not protected is lost (Supplementary Figs. 18, 19). Second, we assume that the relative distribution of human impacts remains constant after protecting a given cell. For example, we assume that fishing effort redistributes across the range of a stock proportionally to the distribution of effort before protection. On the contrary, if fishing effort relocated predominantly towards areas that were previously less-fished, if fishing effort concentrated near the MPAs or if the total fishing effort increased, then our results would probably change. Third, population and recruitment variability were not incorporated into the analysis. MPAs are known to reduce population and

catch variabilities and accounting for these variabilities more explicitly would bolster MPA benefits[39,40]. MPAs also tend to increase the abundance of larger predatory target species, with possible food-web effects[41] that cannot easily be resolved and are beyond the scope of this analysis. Fourth, our results relating to CO_2 released through trawling represent a preliminary best estimate, based on the available data, and further research is required to verify these estimates across scales.

In addition, we recognize that the combination of disparate global datasets introduces uncertainty into our results. Thus, we explore the uncertainty in the biodiversity prioritization in a sensitivity analysis that simulates commission errors in species distributions and adds random noise to feature weights (see Methods, Supplementary Figs. 20–22). Finally, we highlight the need for higher-resolution regional analyses to better resolve priority areas for MPAs at that scale. Our analysis can also be expanded to explicitly model the costs of improved ocean protection[42], and to include additional benefits such as increased tourism revenue[27], improved human well-being[43] and savings due to improved flood and storm-surge protection in coastal habitats[44]. Reduced CO_2 emissions through reduced trawling effort could also generate carbon credits, and provide a meaningful opportunity for financing MPA creation.

Our results may be informative in the context of both national and global conservation targets. The 15th meeting of the Conference of the Parties (COP15) United Nations (UN) Convention on Biological Diversity (CBD), which is to be held in 2021, is expected to produce a global agreement for nature, with an emergent movement to protect at least 30% of the ocean by 2030[45,46] to achieve both biodiversity conservation and climate mitigation goals. Our results lend credence to this target and suggest that a substantial increase in ocean protection could achieve triple benefits—not only protecting biodiversity, but also boosting the productivity of fisheries and securing marine carbon stocks that are at risk from bottom trawling and other industrial activities. Our framework has the flexibility to incorporate the preferences of different governments or stakeholders in identifying priority areas, which can help to motivate a more science-based expansion of ocean protection and contribute to solving three major challenges that face humanity in the twenty-first century—namely, the decline of global biodiversity, the need to provide nutrition to a growing population and the imperative to mitigate climate change. Finally, our framework allows us to identify widespread co-benefits arising from expanded protection that overcome previously perceived trade-offs between biodiversity protection and fisheries.

Online content

Any methods, additional references, Nature Research reporting summaries, source data, extended data, supplementary information, acknowledgements, peer review information; details of author contributions and competing interests; and statements of data and code availability are available at https://doi.org/10.1038/s41586-021-03371-z.

1. Sala, E. & Giakoumi, S. No-take marine reserves are the most effective protected areas in the ocean. *ICES J. Mar. Sci*. **75**, 1166–1168 (2018).
2. Worm, B. et al. Impacts of biodiversity loss on ocean ecosystem services. *Science* **314**, 787–790 (2006).
3. Marine Conservation Institute. The Marine Protection Atlas. http://mpatlas.org (2020).
4. Santos, C. F. et al. Integrating climate change in ocean planning. *Nat. Sustain*. **3**, 505–516 (2020).
5. Costello, C. et al. The future of food from the sea. *Nature* **588**, 95–100 (2020).
6. Brondizio, E.S., Settele, J., Díaz, S. & Ngo, H. T. (eds) *Global Assessment Report on Biodiversity and Ecosystem Services of the Intergovernmental Science-Policy Platform on Biodiversity and Ecosystem Services* (IPBES, 2019).
7. IPCC. *Special Report on the Ocean and Cryosphere in a Changing Climate* https://www.ipcc.ch/srocc/ (2019).
8. Horta e Costa, B. et al. A regulation-based classification system for Marine Protected Areas (MPAs). *Mar. Policy* **72**, 192–198 (2016).
9. Oregon State University, IUCN World Commission on Protected Areas, Marine Conservation Institute, National Geographic Society, & UNEP World Conservation Monitoring Centre. An Introduction to The MPA Guide. https://www.protectedplanet.net/c/mpa-guide (2019).
10. Lester, S. et al. Biological effects within no-take marine reserves: a global synthesis. *Mar. Ecol. Prog. Ser*. **384**, 33–46 (2009).
11. Roberts, C. M. et al. Marine reserves can mitigate and promote adaptation to climate change. *Proc. Natl Acad. Sci. USA* **114**, 6167–6175 (2017).
12. Roberts, C. M. et al. Marine biodiversity hotspots and conservation priorities for tropical reefs. *Science* **295**, 1280–1284 (2002).
13. Selig, E. R. et al. Global priorities for marine biodiversity conservation. *PLoS One* **9**, e82898 (2014).
14. Kuempel, C. D., Jones, K. R., Watson, J. E. M. & Possingham, H. P. Quantifying biases in marine-protected-area placement relative to abatable threats. *Conserv. Biol*. **33**, 1350–1359 (2019).
15. McGowan, J. et al. Prioritizing debt conversions for marine conservation. *Conserv. Biol*. **34**, 1065–1075 (2020).
16. Halpern, B. S. et al. Spatial and temporal changes in cumulative human impacts on the world's ocean. *Nat. Commun*. **6**, 7615 (2015).
17. Lenoir, J. et al. Species better track climate warming in the oceans than on land. *Nat. Ecol. Evol*. **4**, 1044–1059 (2020).
18. Tittensor, D. P. et al. Integrating climate adaptation and biodiversity conservation in the global ocean. *Sci. Adv*. **5**, eaay9969 (2019).
19. Kaschner, K. et al. AquaMaps: predicted range maps for aquatic species. Version 08/2016c https://www.aquamaps.org/ (2016).
20. Riahi, K. et al. RCP 8.5—a scenario of comparatively high greenhouse gas emissions. *Clim. Change* **109**, 33 (2011).
21. Nakicenovic, N. et al. *Special Report on Emissions Scenarios (SRES): a Special Report of Working Group III of the Intergovernmental Panel on Climate Change* (Cambridge Univ. Press, 2000).
22. Goñi, R., Badalamenti, F. & Tupper, M. H. in *Marine Protected Areas: A Multidisciplinary Approach* (ed. Claudet, J.) 72–98 (Cambridge Univ. Press, 2011).
23. Halpern, B. S., Lester, S. E. & Kellner, J. B. Spillover from marine reserves and the replenishment of fished stocks. *Environ. Conserv*. **36**, 268–276 (2009).
24. Lynham, J., Nikolaev, A., Raynor, J., Vilela, T. & Villaseñor-Derbez, J. C. Impact of two of the world's largest protected areas on longline fishery catch rates. *Nat. Commun*. **11**, 979 (2020).
25. Gaines, S. D., Lester, S. E., Grorud-Colvert, K., Costello, C. & Pollnac, R. Evolving science of marine reserves: new developments and emerging research frontiers. *Proc. Natl Acad. Sci. USA* **107**, 18251–18255 (2010).
26. Hastings, A. & Botsford, L. W. Equivalence in yield from marine reserves and traditional fisheries management. *Science* **284**, 1537–1538 (1999).
27. Costello, C. et al. Global fishery prospects under contrasting management regimes. *Proc. Natl Acad. Sci. USA* **113**, 5125–5129 (2016).
28. Cabral, R. B. et al. A global network of marine protected areas for food. *Proc. Natl Acad. Sci. USA* **117**, 28134–28139 (2020).
29. Atwood, T. B., Witt, A., Mayorga, J., Hammill, E. & Sala, E. Global patterns in marine sediment carbon stocks. *Front. Mar. Sci*. **7**, 165 (2020).
30. Estes, E. R. et al. Persistent organic matter in oxic subseafloor sediment. *Nat. Geosci*. **12**, 126 (2019).
31. Griscom, B. W. et al. Natural climate solutions. *Proc. Natl Acad. Sci. USA* **114**, 11645–11650 (2017).
32. Metz, B., Davidson, O. de Coninck, H., Loos, M., & Meyer, L. (eds) *IPCC Special Report on Carbon Dioxide Capture and Storage* (Cambridge Univ. Press, 2005).
33. Gruber, N. et al. The oceanic sink for anthropogenic CO_2 from 1994 to 2007. *Science* **363**, 1193–1199 (2019).
34. Davidson, E. A. & Ackerman, I. L. Changes in soil carbon inventories following cultivation of previously untilled soils. *Biogeochemistry* **20**, 161–193 (1993).
35. Legge, O. et al. Carbon on the Northwest European shelf: contemporary budget and future influences. *Front. Mar. Sci*. **7**, 143 (2020).
36. Pusceddu, A. et al. Chronic and intensive bottom trawling impairs deep-sea biodiversity and ecosystem functioning. *Proc. Natl Acad. Sci. USA* **111**, 8861–8866 (2014).
37. Beger, M. et al. Integrating regional conservation priorities for multiple objectives into national policy. *Nat. Commun*. **6**, 8208 (2015).
38. Montesino Pouzols, F. et al. Global protected area expansion is compromised by projected land-use and parochialism. *Nature* **516**, 383–386 (2014).
39. Mangel, M. Irreducible uncertainties, sustainable fisheries and marine reserves. *Evol. Ecol. Res*. **2**, 547–557 (2000).
40. Rodwell, L. D. & Roberts, C. M. Fishing and the impact of marine reserves in a variable environment. *Can. J. Fish. Aquat. Sci*. **61**, 2053–2068 (2004).
41. Caselle, J. E., Rassweiler, A., Hamilton, S. L. & Warner, R. R. Recovery trajectories of kelp forest animals are rapid yet spatially variable across a network of temperate marine protected areas. *Sci. Rep*. **5**, 14102 (2015).
42. McCrea-Strub, A. et al. Understanding the cost of establishing marine protected areas. *Mar. Policy* **35**, 1–9 (2011).
43. Ban, N. C. et al. Well-being outcomes of marine protected areas. *Nat. Sustain*. **2**, 524 (2019).
44. Barbier, E. B., Burgess, J. C. & Dean, T. J. How to pay for saving biodiversity. *Science* **360**, 486–488 (2018).
45. O'Leary, B. C. et al. Effective coverage targets for ocean protection. *Conserv. Lett*. **9**, 398–404 (2016).
46. Roberts, C. M., O'Leary, B. C. & Hawkins, J. P. Climate change mitigation and nature conservation both require higher protected area targets. *Phil. Trans. R. Soc. Lond. B* **375**, 20190121 (2020).

Methods

Data

We used the best available spatial data layers comprising current species distributions (n = 4,242), projected species distributions (n = 4,242), marine sedimentary carbon stocks (n = 1), seamount density distributions (n = 194), coastal, pelagic, abyssal and bathyal biogeographical provinces (n = 127), commercially exploited fish and invertebrate stocks (n = 1,150), and human impacts on the world's oceans (n = 70). We harmonized all data layers with a Mollweide equal-area projection (around 50 km × 50 km), and these were cropped to ocean areas using a 1:50 m land mask obtained from https://www.naturalearthdata.com. All data processing was done in R using rgdal, raster, sf and tidyverse libraries.

Species list and distributions

We constrained our analysis to consider those species that are (1) directly or indirectly affected by threats abatable by MPAs as reported by the International Union for Conservation of Nature (IUCN) or (2) reported in global catch databases[47,48]. The resulting dataset contains 5,405 species, 30% of which are directly targeted by fisheries. We obtained species distribution information as the probability of occurrence in each spatial cell on the basis of environmental variables and constrained by currently known natural ranges[19]. Distributions for seabirds were obtained directly from BirdLife International (http://datazone.birdlife.org/home). Species distributions were available at a 0.5° resolution, and were subsequently rasterized, re-projected to a Mollweide equal-area projection and normalized such that the values across a species range add up to one. Overall, species distribution data were available for 4,242 (78%) of the species in the initial list representing all major taxonomic groups: Osteichthyes (n = 2,115), Chondrichthyes (n = 760), Cnidaria (n = 586), Mollusca (n = 205), Arthropoda (n = 201), Aves (n = 173), Mammalia (n = 111), Echinoderms (n = 39) and Reptilia (n = 18) (Supplementary Figs. 23–25, Supplementary Table 1).

Seamounts

We include seamounts in our analysis as they are known aggregators of pelagic biodiversity and an important habitat for deep-sea species that are still underrepresented in global species distribution datasets[49]. We used the spatial locations of 10,604 of the world's bathyal seamounts (below 3,500 m) classified into 194 classes based on four biologically relevant characteristics: overlying export production, summit depth, oxygen level and proximity[50] (Supplementary Fig. 26). For each seamount class, we created a raster layer with the number of seamounts in each grid cell, which we normalized to obtain the fraction of total seamounts per unit area. Each class of seamounts was treated as an individual feature in the analysis.

Biogeographical provinces

We used the spatial delineations of the pelagic (n = 37), coastal (n = 62), bathyal (n = 14), and abyssal (n = 14) provinces of the ocean as individual biodiversity features to ensure representation of different facets of biodiversity throughout the world's ocean[51–53]. These provinces have been delineated on the basis of the best available oceanographic and biological data along with expert consultation and are thought to contain biogeographically distinct assemblages of species and communities with a shared evolutionary history (Supplementary Figs. 28, 29). Spatial polygons were converted to rasters by estimating the fraction of each pixel covered by each province for province polygons that overlapped the centre of the pixel.

Food provisioning

We used data for 1,150 commercially exploited fish and invertebrate stocks—which have an associated MSY of 56.6 MMT—to model their response to MPAs and the resulting change in future catch in remaining fishing areas after protection[28]. Because global MSY is at least 80 MMT[27], and stocks not included in our analysis are probably in worse shape than the stocks for which we have requisite data, we can conservatively scale up the food provisioning potential from MPAs by 41%.

We define the food provisioning potential of a given network of MPA (s) as the change in total future catch that is due to the MPA network s; that is, $\Delta H_s = \Sigma_j H_{s,j} - \Sigma_j H_{\text{bau},j}$, where $H_{s,j}$ is the catch of stock j given MPA network s and $H_{\text{bau},j}$ is the catch of stock j with no additional MPAs (or business-as-usual; bau).

We model the biomass transitions of each individual stock j inside ($B_{\text{in},j}$) and outside ($B_{\text{out},j}$) MPAs as

$$B_{\text{in},j,t+1} = B_{\text{in},j,t} + R_j r_j (B_{\text{in},j,t} + B_{\text{out},j,t})\left(1 - \frac{B_{\text{in},j,t} + B_{\text{out},j,t}}{K_i}\right) - m_j(1 - R_j)\left(B_{\text{in},j,t} - \frac{R_j}{1 - R_j} B_{\text{out},j,t}\right) \quad \text{and}$$

$$B_{\text{out},j,t+1} = (1 - E_{j,t})B_{\text{out},j,t} + (1 - R_j) r_j (B_{\text{in},j,t} + B_{\text{out},j,t})\left(1 - \frac{B_{\text{in},j,t} + B_{\text{out},j,t}}{K_j}\right) + m_j(1 - R_j)\left(B_{\text{in},j,t} - \frac{R_j}{1 - R_j} B_{\text{out},j,t}\right),$$

where t is time, r_j is intrinsic growth rate, K_j is carrying capacity, m_j is species relative mobility, R_j is the proportion of stock's carrying capacity in MPAs and E_j is the exploitation rate.

The catch of stock j at each time step is given by $H_{j,t} = E_{j,t} B_{\text{out},j,t}$ and the steady-state catch is given by

$$H_j = E_j \left(\frac{m_j K_j (1 - R_j)}{E_j R_j + m_j}\right)\left(1 - \frac{E_j (1 - R_j) m_j}{(E_j R_j + m_j) r_j}\right).$$

We derive the intrinsic growth rate (r) of individual stocks from Thorson[54], FishBase[55] and SeaLifeBase[56]. We combine the MSY estimate per stock from a previous study[27] with our compiled growth rates to calculate the total carrying capacity per stock. We consistently used species-specific intrinsic growth rates in our model regardless of the region, as regional variations in growth rates for over a thousand stocks are not available. We distribute the total carrying capacity in space in proportion to the stock's probability of occurrence from AquaMaps species' native ranges[19]. Finally, we derive species relative mobility (m) by categorizing stocks based on the linear scales of movement of adult individuals: m = 0.1 represents species with maximum scales of movement of less than 1 km, m = 0.3 represents species with maximum scales of movement of between 1–50 km, and m = 0.9 represents species with maximum scales of movement of more than 50 km. Other parameters for evaluating MPA effects on catch are generated dynamically, such as the proportion of stock range under protection (R).

Carbon

We used a published modelled spatial layer of global marine carbon stocks stored in the first metre of ocean sediment based on a sample of 11,578 sediment cores collected throughout the global ocean[29] (Supplementary Fig. 30). The data layer was resampled using bilinear interpolation and re-projected from its original 1-km^2 resolution to match our working resolution and equal-area projection.

Administrative data

We use the Marine Protection Atlas database[3] to select MPAs that are classified as fully or highly protected (that is, no-take MPAs or protected areas in which only minimal subsistence or recreational fisheries are allowed), and that have been implemented as of September 2020. The resulting dataset consists of 1,398 MPAs, covering 2.7% of the world's ocean. Lastly, we used the political boundaries of the world's EEZs as made available by https://marineregions.org/ (v.10).

Biodiversity benefit

A schematic diagram for calculating benefits for each objective is shown in Supplementary Fig. 31. For biodiversity, we include 4,559 individual features corresponding to: (1) species' native ranges, extinction risk and functional and evolutionary distinctiveness for 4,242 marine species that are directly or indirectly affected by fishing[19]; (2) density of seamounts grouped into 194 distinct classes[50]; and (3) 37 pelagic, 62 coastal, 14 abyssal and 14 bathyal biogeographical provinces[53,57]. For each feature, we use benefit functions resembling species–area relationships to capture the diminishing marginal benefit from additional protection.

We define the biodiversity benefit (B) of protecting a set of pixels (s) as

$$B_s = \sum_j \sigma_j (X_{j_s})^{z_j},$$

where σ_j represents the weight given to feature j and z_j is the curvature of a power function analogous to a species–area curve. X_{j_s} corresponds to the fraction of the total suitable habitat of feature j that remains viable given the set of protected pixels (s), and is defined as

$$X_{j_s} = \sum_{i \in s} \upsilon_{i,j}^{\text{in}} + \sum_{i \notin s} \upsilon_{i,j}^{\text{out}},$$

where $\upsilon_{i,j}^{\text{in}}$ and $\upsilon_{i,j}^{\text{out}}$ correspond to the fraction of the feature's total habitat that remains suitable in pixel i if i is protected, and if pixel i is left unprotected, respectively. These are defined as

$$\upsilon_{i,j}^{\text{in}} = \upsilon_{i,j_0}^{\text{in}}(1 - I_{u_i}) \text{ and}$$

$$\upsilon_{i,j}^{\text{out}} = \upsilon_{i,j_0}(1 - I_{u_i})(1 - I_{a_i}),$$

where υ_{i,j_0} represents the current fraction of a feature's total suitable habitat present in pixel i, I_{u_i} is the fraction of that habitat that may be lost owing to un-abatable impacts and I_{a_i} is the fraction of that habitat that may be lost as a result of abatable impacts[13] (Supplementary Figs. 17–19). The term 'feature' refers to an individual species, a class of seamount, or a biogeographical province.

We estimate I_{a_i} and I_{u_i} using the most recent five years (2009–2013) of human impacts on the world's ocean[58]. Data were classified into impacts that are abatable (artisanal fishing, commercial fishing classified in pelagic high-by-catch, pelagic low-by-catch, demersal destructive, demersal non-destructive high by-catch, and demersal non-destructive low by-catch) and those that are un-abatable (sea surface temperature rise, light pollution, organics and nutrient pollution, ocean acidification, shipping, and sea-level rise) in relation to MPAs. Human impact layers were resampled using bilinear interpolation to match our working resolution. To estimate the fraction of suitable habitat lost we assume a saturating relationship rescaled between 0–1 such that

$$I_{a_i} = \frac{\log(\sum_{k=1}^{K} I_{k,i}) - \min(\log(\sum_{k=1}^{K} I_{k,i}))}{\max(\log(\sum_{k=1}^{K} I_{k,i})) - \min(\log(\sum_{k=1}^{K} I_{k,i}))}; \forall\, k \in \text{abatable}$$

$$I_{u_i} = \frac{\log(\sum_{k=1}^{K} I_{k,i}) - \min(\log(\sum_{k=1}^{K} I_{k,i}))}{\max(\log(\sum_{k=1}^{K} I_{k,i})) - \min(\log(\sum_{k=1}^{K} I_{k,i}))}; \forall\, k \notin \text{abatable},$$

where $I_{k,i}$ is the average impact of stressor k in pixel i in the last five years, and K is the total number of stressor layers in the model ($n = 16$). The human impacts dataset already accounts for the differential effects of a stressor in different ecosystems and environmental conditions (for example, ocean productivity). Ideally one would incorporate the differential effects across species. However, given the current limited state of knowledge regarding species-response curves to different stressors, we assume that the abatable and un-abatable impacts in a pixel affect all features in that pixel equally.

We weighted the species in the analysis as a function of their extinction risk (EX)[59], functional distinctiveness (FD) and evolutionary distinctiveness (ED). These weights are calculated using additive and multiplicative components as proposed previously[60]:

$$\sigma_j = \text{EX}_j(\text{FD}_j + \text{ED}_j)\ ; \forall\, j \in \text{species}.$$

Following a previous report[38], we numerically coded the IUCN classification of extinction risk such that the highest weight is given to critically endangered species (least concern = 1; near-threatened = 2; vulnerable = 4; endangered = 6; critically endangered = 8; data deficient = 2). Unassessed species were treated as data-deficient, and the numerical values were normalized so that the maximum weight equals 1.

For each taxonomic class, we used a set of functional traits and a phylogeny to estimate species functional and evolutionary distinctiveness, respectively, for fishes[61], sharks[62], marine mammals[63], birds[64]. We computed the functional distance between all pairs of species within a given taxonomic class using the compute_dist_matrix function in the funrar R package. Functional distinctiveness FD_i of species i represents the extent to which the traits of species i are distinct relative to the traits of all the other species from the same taxonomic class at a global scale[65]:

$$\text{FD}_i = \frac{\sum_{j=1; j \neq i}^{N} d_{i,j}}{N - 1},$$

where $d_{i,j}$ is the functional distance between species i and j, and N is the total number of species. The functional distances $d_{i,j}$ are scaled between 0 and 1 (maximum value), so FD_i is 0 when all species have the same trait values (the functional distance between all species pairs is 0), and 1 when species i is maximally differentiated from all other species. This calculation was carried out using the distinctiveness function in the funrar R package. Using the same approach, we also estimated species evolutionary distinctiveness. The evolutionary distinctiveness of species i, ED_i, is high when the species has a long unshared branch length with all the other species. The more 'isolated' a species is in a phylogenetic tree, the higher its evolutionary distinctiveness. We computed ED using the evol.distinct function from the picante R package. We did not have enough information to estimate functional and evolutionary distinctiveness for 15% of the species in the analysis. We imputed these values using arithmetic means for each taxonomic class when possible, and sample means when entire classes lacked data (for example, Reptilia). For seamounts, we weighted each class the same, such that the aggregate weight given to all seamounts equalled the aggregate weight given to all species. The same weighting approach was applied to the biogeographical provinces.

The parameter z_j, which determines the curvature of the power function and is analogous to the exponent of a species-area curve, was set equal to 0.25 for all features, based on a typical species-area relationship z-value between 0.2 and 0.3[66]. The rationale behind a benefit function with exponent z_j is that there is a relationship between area lost (that is, not protected) and a species' risk of extinction. The parameterization of z_j will depend on a species' characteristics and other information, including scale of movement (for which z decreases with higher movement[67]), trophic level (for which z increases with trophic rank[68]) and human impacts (for which z decreases with higher exploitation[69]), amongst other things. A feature-specific z_j would therefore theoretically be preferred, but in the absence of a systematic method for parameterizing z for all features in our analysis, we test a range of constant z-values

($z = 0.1, 0.2, 0.3, 0.4$). Although z is important to determine the biodiversity benefits under business-as-usual and thus the magnitude of the MPA effect on biodiversity persistence, the normalized global benefits accruing from protection are relatively insensitive to the value of this parameter (Supplementary Figs. 32, 33). We used the Kendall tau correlation coefficient—a nonparametric statistic that measures the similarity in the ordering of the rankings—to compare the top 30% of the solutions using $z = 0.1$ and $z = 0.4$, and found that the results are robust to z ($\tau = 0.95$).

Food provisioning benefit

The food provision benefit (F) is defined as the difference in catch made by an additional set of fully protected pixels or MPAs (s); that is, the difference between the global catch with and without implementing additional MPAs. F is estimated at equilibrium such that:

$$F_s = \left[\sum_j E_{s,j}\left(\frac{m_j K_j(1-R_{s,j})}{E_{s,j}R_{s,j}+m_j}\right)\left(1-\frac{E_j(1-R_{s,j})m_j}{(E_{s,j}R_{s,j}+m_j)r_j}\right)\right] -$$

$$\left[\sum_j E_{\mathrm{bau},j}\left(\frac{m_j K_j(1-R_{\mathrm{bau},j})}{E_{\mathrm{bau},j}R_{\mathrm{bau},j}+m_j}\right)\left(1-\frac{E_{\mathrm{bau},j}(1-R_{\mathrm{bau},j})m_j}{(E_{\mathrm{bau},j}R_{\mathrm{bau},j}+m_j)r_j}\right)\right],$$

where m_j represents the mobility of stock j, K_j is total carrying capacity, $R_{s,j}$ is the fraction of total K that is inside the set of protected cells (s) and r_j represents the stock growth rate. The parameters $E_{s,j}$ and $E_{\mathrm{bau},j}$ pertain to the equilibrium exploitation rate of stock j in the fishing area in the presence of an MPA network (s) and in the absence of additional MPAs, respectively. We derived the exploitation rate per stock in a world with no MPAs ($E_{0,j}$) using the 'conservation concern' business-as-usual scenario of a previous study[27]. This scenario assigns future fisheries prospects according to current stock status and management as follows: (i) for assessed stocks, current exploitation rates are held constant in perpetuity; (ii) for unassessed stocks of 'conservation concern' (that is, those currently overfished or experiencing overfishing), open-access dynamics are assumed; and (iii) for unassessed, non-conservation concern stocks, the exploitation rate is set to maintain current biomass. We then solve for the exploitation rate per stock in the fishing area given currently implemented MPAs and given our prioritized network of MPAs (s) by accounting for fishing effort redistribution (see below).

Fishing effort redistribution

We considered two common fishing effort redistribution models: (1) all fishing effort in areas designated as MPAs will transfer to the remaining fishing areas (full-effort transfer); and (2) fishing effort in areas designated as MPA will go away and the fishing effort density in fishing area remains the same (no-effort transfer). If fishing effort displaces after protection, it does so such that the relative levels of fishing outside remain constant. We assume that effort redistributes across the range of a stock proportionally to the distribution of effort before protection. With full-effort transfer, the fishing mortality of a stock outside an MPA increases in proportion to the size of the MPA, that is, the new fishing mortality equals $1/(1 - R_{s,j})$ times the fishing mortality with no additional MPA[70–73]. The exploitation rate (E) can be expressed in terms of fishing mortality as $E = 1 - e^{-F}$. Hence, the exploitation rate per stock in fishing area given the current MPAs and given a network of MPAs (s) is given by $E_{\mathrm{bau},j} = 1 - (1 - E_{0,j})^{1/(1-R_{\mathrm{bau},j})}$ and $E_{s,j} = 1 - (1 - E_{0,j})^{1/(1-R_{s,j})}$, respectively. Under the no-effort transfer assumption, the exploitation rate experienced by the stock biomass outside the MPA remains the same (that is, $E_{\mathrm{bau},j}$) after MPA implementation. Supplementary Figure 34 shows the results of both models. The potential food provisioning benefit is slightly lower under the no-effort redistribution assumption primarily because the total catches from underfished and well-managed fisheries are lower compared to the full-effort redistribution scenario in which fishers would try to compensate for the harvest lost from MPAs by increasing fishing effort in the remaining fishing areas.

Carbon benefit

We defined the carbon benefit (C) as a linear function of the amount of carbon that remains given a set of protected areas (s), such that:

$$C_s = X_{C_s} \text{ and}$$

$$X_{C_s} = \sum_{i \in s} c_i^{\mathrm{in}} + \sum_{i \notin s} c_i^{\mathrm{out}},$$

where c_i^{in} and c_i^{out} correspond to the fraction of total carbon that remains in pixel i if i is protected, and if pixel i is left unprotected, respectively. We estimate c_i^{in} and c_i^{out} using the same approach as in the biodiversity benefit but without un-abatable impacts such that:

$$c_i^{\mathrm{in}} = c_{i_0} \text{ and}$$

$$c_i^{\mathrm{out}} = c_{i_0}(1 - I_{a_i}),$$

where c_{i_0} is the estimated carbon stored in the first meter of sediment in pixel i, and I_{a_i} is the fraction of that carbon that would be lost (that is, remineralized to aqueous CO_2) in the absence of protection. The latter is estimated as:

$$I_{a_i} = \mathrm{SVR}_i \times p_{\mathrm{crd}_i} \times p_{\mathrm{lab}_i} \times (1 - e^{-k_i t}),$$

where SVR_i (swept volume ratio) is the fraction of the carbon in pixel i that is disturbed by bottom trawling and dredging fishing practices, p_{crd_i} is the proportion that resettles in pixel i after disturbance, p_{lab_i} is the fraction of carbon that is labile, k_i is the first-order degradation rate constant and t represents time, which is set to one year.

The SVR_i from fishing is estimated by:

$$\mathrm{SVR}_i = \sum_g \mathrm{SAR}_{i,g} \times p_{\mathrm{depth}_g},$$

where $\mathrm{SAR}_{i,g}$ is the swept area ratio of pixel i by vessels using gear g, and p_{depth_g} is the average penetration depth of gear type g. $\mathrm{SAR}_{i,g}$ is estimated as follows:

$$\mathrm{SAR}_{i,g} = \frac{\sum_v^V \mathrm{TD}_{i,v} \times W_v}{A_i},$$

where $\mathrm{TD}_{i,v}$ is the trawled distance by vessel v in pixel i, W_v is the width of the gear trawled by vessel v and A_i is the total area of pixel i. Trawled distance (TD) is estimated using fishing activity detected by automatic identification systems (AIS) data from Global Fishing Watch (GFW) between 2016 and 2019. For each vessel v in each cell i, TD is the sum of the product between time and speed across all AIS positions associated with fishing activity in pixel i (see ref. [74] for more details on detecting fishing activity from AIS). We include only those fishing vessels that are registered as—or have been classified by GFW as—trawlers or dredgers. We used official fishing registries from the European Union and the Convention for the Conservation of Antarctic Marine Living Resources (CCAMLR) to refine this classification into five gear types: otter trawls, beam trawls, towed dredges, hydraulic dredges and midwater trawls. Vessels classified as midwater trawls were excluded entirely from this analysis, because this gear type does not come into contact with the seafloor. Vessels without official classification were classified as otter trawls as these are the most common type of bottom trawlers in the ocean. Finally, to minimize noise and AIS positions misclassified as fishing, we include only fishing positions within the range of common

depths and speeds reported for each gear type by Eigaard et al.[75]: otter trawls, towing speeds of 2–4 knots and depths up to 2,000 m; beam trawls, towing speeds of 2.5–7 knots and depths up to 100 m; towed and hydraulic dredges, towing speed of 2–2.5 knots.

The width of the trawled gear of each vessel W_v was estimated using vessel-size-footprint relationships reported by Eigaard et al.[75], such as:

$$W_{(TD;HD)} = 0.3142 \times LOA^{1.2454}$$

$$W_{(OT)} = 10.6608 \times KW^{0.2921}$$

$$W_{(BT)} = 0.6601 \times KW^{0.5078}$$

where LOA is the vessel's length overall in meters, and KW is its engine power. Within each gear type, there is variability in gear dimension based on target species and other factors. Because we do not have data on the target species of each vessel, we use the relationships reported in Eigaard et al.[75] to specify gear dimension as that associated with the largest variety of target species. We estimate that on average, a total of 4.9 million km^2 of the ocean is trawled each year. This represents around 1.3% of the total ocean area.

The remaining parameters were obtained from the scientific literature. We used the average penetration depths reported by Hiddink et al.[76] for otter trawls (2.44 cm), beam trawls (2.72 cm), towed dredges (5.47 cm) and hydraulic dredges (16.11 cm). Of these gear types, otter trawlers are the most prominent, with an average area fished of 4.65 million km^2 per year. As a result, the area-weighted average sediment penetration depth across all gear types corresponds to 2.44 cm. The fraction of carbon in each cell that resettles in that same cell after trawling (p_{crd_i}) was assumed constant at 0.87, and was estimated using the average from studies that quantified the amount of sediment load lost following trawling or mining[77–81]. For this study we focused only on the proportion of carbon that is labile (p_{lab_i}), and thus more prone to remineralization after a disturbance. The labile fraction was estimated as a function of the type of sediment. We used sediment type as a proxy for estimating the amount of labile carbon because it relates to many aspects that can influence the preservation and remineralization of organic matter (for example, oxygen penetration depths, permeability, infaunal communities[82,83] and physical protection[84]), as well as reflect its origin[85]. The proportion of labile carbon assigned to each sediment type was estimated using literature values that were tuned to our model[86,87]; pixels dominated by 'fine' sediments such as muds, silts or biogenic (more than 50% of pixel area) were assigned a $p_{lab_i} = 0.7$, those dominated by 'coarse' sediments like gravel (more than 50%) a $p_{lab_i} = 0.286$, and the remaining combinations of 'sandy' sediments were assigned a $p_{lab_i} = 0.04$. We classified pixel sediment types using the sediment lithology from a previous study[72], grouped as follows: coarse: gravel, coarse sediments, ash-volcanic, shells and coral fragments; sandy: sand and fine-grained calcareous sediment; fines: silt, clay and siliceous mud; biogenic: radiolarian ooze, diatom ooze, mix calcareous-siliceous ooze, siliceous ooze and calcareous ooze.

The first-order degradation rate constants (k_i) were assigned as a function of oceanic region, and were estimated from ranges of values presented in the literature for oxic sediments that were then tuned to our model[86,87]; North Pacific = 1.67, South Pacific = 3.84, Atlantic = 1.00, Indian = 4.76, Mediterranean = 12.3, Arctic = 0.275, Gulf of Mexico and Caribbean = 16.8. Values for the North and South Atlantic, as well as the Gulf of Mexico and the Caribbean, were combined owing to the paucity of studies in the South Atlantic and the Caribbean. We included only oxic sediments in our model because one of our main assumptions about physical disturbances to marine sediments, such as benthic fishing, is that mixing of the sediments and resuspension increases the amount of time the disturbed carbon is in contact with oxygen[88].

Finally, to avoid the random ranking of pixels without bottom trawling but with different amounts of carbon, we assigned a small and constant $I_a = 10^{-30}$ to each pixel without trawling data. To be as precise as possible, we performed the analysis to estimate the annual CO_2 efflux at a 1-km resolution. This minimizes the risk of overestimation due to a coarse scale. However, to harmonize the carbon analysis with biodiversity and food provision, we ran the carbon model at a 50 km × 50-km resolution in all multi-objective prioritizations. As a result, we probably overestimate the total area in which trawling is occurring and subsequently the total area needed to safeguard carbon stocks. On the other hand, although the GFW database is the most comprehensive publicly available source of fishing effort data, it does not account for every single bottom trawler in the world and lacks fishing effort data for thousands of fishing vessels that do not carry AIS, predominantly from developing nations.

Finally, to report the total benthic annual CO_2 efflux (Mg CO_2), we estimate the efflux in a given pixel i as:

$$CO_{2_i} = w \times c_{0_i} \times I_{a_i},$$

where c_{0_i} is the carbon stored in the first meter of sediment in pixel i, I_{a_i} is the is the fraction of that carbon that would be lost in the absence of protection (as defined above) and w is the ratio of the weight of CO_2 relative to that of C (that is, 3.67 tons of CO_2 equal to 1 ton of C).

Overall, we found that the average carbon stock in sediments disturbed by bottom trawling is 9.1×10^3 Mg C km^{-2} (global average is 6.6×10^3 Mg C km^{-2}). The average remineralization efficiency of disturbed carbon—estimated as the mean across pixel level remineralization rates—is 29.7%.

Carbon model validation

Cross-comparisons of our model results for the effects of trawling on CO_2 efflux from the sediment–water interface are difficult because of the novelty of this topic. Although several studies have documented increased benthic metabolism after trawling, most of these studies have measured changes in oxygen or variables other than CO_2 efflux. Furthermore, the studies that have measured CO_2 efflux from the sediment-water interface are non-spatial in nature. To validate our model, we compared our predicted values with measured CO_2 annual efflux values either from studies that explicitly measured CO_2 efflux at the sediment–water interface from trawled sediments, or from benthic metabolism studies that were conducted in areas in which trawling occurs. In all cases, studies provided only descriptions of site locations or coarse GPS coordinates. As a result, we compared the measured value from the study with an average predicted value for the study location. In total, we found four studies that met our criteria for comparisons (See Supplementary Table 2). Our predicted CO_2 annual efflux values are of the same order of magnitude and underestimate the reported values. The root-mean-square error of the predicted values is 0.004×10^9 mol CO_2 km^{-2} and a log-transformed linear regression yields $R^2 = 0.79$.

Effects of multiple years of trawling on carbon efflux

Let C_t be the total carbon in the first metre of the sediments affected by bottom trawling. Assuming that the footprint and intensity of bottom trawling remains constant every year, we model net carbon depletion as: $C_{t+1} = C_t + CA_t - CL_t$, where C_t is the carbon stock in time t, CA_t is the annual addition of carbon from external sources and CL_t is the carbon lost each year. The carbon stocks in trawled sediments in year zero (C_0) are 54.89×10^9 Mg C (from this analysis), and the annual addition of carbon into trawled areas from external sources amounts to 96.04×10^6 Mg C, which we calculate as the product of the total area trawled (4.9×10^6 km^2; from this analysis) and the average carbon accumulation rates for coastal shelf systems (19.6 Mg C km^{-2} yr^{-1}) (ref. [89]).

The annual carbon lost each year as a result of trawling comprises: (1) carbon that is resuspended into the water column and then laterally

transported to a different pixel where its fate is unknown (CT); and (2) carbon that is remineralized in the sediment (CR). Thus $CL_t = CT_t + CR_t$, where $CT_t = C_d(1 - pcrd)$, and $CR_t = C_d\epsilon$, where pcrd is the fraction of disturbed sediment that resettles (pcrd = 0.87), and ϵ is the remineralization efficiency of disturbed sediments ($\epsilon = 0.3$, from our analysis). C_d corresponds to the carbon that is disturbed each year by trawling, which we define as:

$$C_{d,t} = C_{d,t-1} - CT_{t-1} - CR_{t-1} + C_n + CA_t,$$

where C_n is the newly available labile carbon that comes from deeper sediment layers that have become recently exposed by trawling-induced erosion in year. This is estimated as the difference between the average trawl penetration depth (pd = 2.44 cm) and the depth of sediment resettled after previous trawling; accounting for natural sediment accumulation rates (rs = 0.07 cm yr^{-1} for coastal shelf systems[90]): $C_n = C_0(pd - pd \times pcrd - rs)$. This yields an annual deepening of the disturbed carbon layer of 0.0024 m yr^{-1}.

This analysis suggests it would take around 400 years for trawling (at its current scale and intensity) to exhaust all of the sediments in the top 1 m. Moreover, we find that remineralization rates stabilize at 40% of the initial rate after the 9th successive year of constant trawling (Supplementary Fig. 35). Our assumptions are that carbon losses and additions are constant year to year, carbon stocks are equally distributed in the top metre of sediment, carbon stocks stored in sediment deeper than that which is directly affected by the trawl are unaffected, and that each pixel where there is bottom trawling is disturbed once a year.

Ranking algorithm

We implemented a heuristic, forward-looking algorithm to iteratively select pixels that maximize our defined benefit functions at each step. This approach builds on the existing and widely used zonation algorithm[60] but differs in two important ways. First, our approach does not impose the constraint that protecting the entire world is best, which enables us to use non-monotonic benefit functions, such as the one for food provisioning. Second, our algorithm can account for the value of unprotected cells, which allows us to base benefit functions on the entire landscape, not only on those cells selected for protection. Using the biodiversity objective as an example, the algorithm operates as follows:

1. Compute starting conditions. Given the current protected areas and the distribution of human impacts, estimate the biodiversity benefit for every feature under business as usual.
2. Set rank $r = 0$.
3. Estimate the marginal increase in benefit δB from protecting each pixel i:

$$\delta B_i = B_{s_0+i} - B_{s_0}$$

$$\delta B_i = \sum_j \sigma_j (X_{j_{s0}+i})^z - \sum_j \sigma_j (X_{j_{s0}})^z,$$

which can be approximated as

$$\delta B_i \approx \sum_j \sigma_j \Delta X_{j_i} S_{j_0}$$

$$\delta B_i \approx \sum_j \sigma_j (v_{i,j}^{in} - v_{i,j}^{out}) S_{j_0}$$

where S_{j_0} is the derivative of the benefit function with respect to X_j at any given step.

4. Select the pixel k that maximizes δB and assign it a rank of $r = r + 1$.
5. Update current conditions.
6. Return to step 3 until all pixels have been selected.

Note that at any given step, the slope S_{j_0} is independent of the pixel i that is being evaluated for selection, and thus it needs to be estimated only once for each feature[91]. Furthermore, for a given feature, the decision to select a pixel depends only on the pixel-specific difference in value with and without protection, which in turn depends on the relative levels of abatable and un-abatable impacts such that:

$$v_{i,j}^{in} - v_{i,j}^{out} = v_{i,j_0}(1 - I_{u_i})I_{a_i}.$$

It is this interaction between types of impacts in a given cell that gives higher priority to areas in which abatable impacts are relatively high and un-abatable impacts are relatively low.

Given the global scale of this analysis, we made the simplifying assumption that the costs to establish, implement and manage MPAs are uniform. Realistic, comprehensive and spatially explicit datasets that account for variations in these costs for MPAs are not available at present. However, when possible, such data can and should be integrated into our prioritization framework at scales relevant for conservation planning[92–94].

Multi-objective prioritization

We jointly maximize multiple objectives for biodiversity, carbon and food by combining them into a single benefit function such that the utility of a set of protected pixels (U_s) can be defined as:

$$U_s = \alpha_b B_s + \alpha_c C_s + \alpha_f F_s,$$

where α_b, α_c and α_f correspond to the weights given to the biodiversity, carbon and food objectives, respectively, which in turn reflect our preferences for each of the three goals. As there is no globally accepted weighting scheme to aggregate our three goals, any multi-objective optimization will be subjective. To illustrate the possibilities without imposing our own subjectivity, we explore how the optimal level of ocean protection to maximize net benefits changes given different preferences. For this analysis, we vary the weight given to biodiversity across a range of −100× to 100× the weight placed on food provisioning. For example, a weight of 1 would mean that the value of reaching the maximum biodiversity benefits is equal to the value of the maximum change in catch (5.9 MMT). A value of 0.5 would indicate that food provisioning is twice as valuable as biodiversity, and a value of −1 would imply that by reaching maximum biodiversity benefits we would incur a loss comparable to losing 5.9 MMT of catch. For this exercise we treat carbon as a co-benefit and assign it a weight of zero.

Incorporating climate change

We framed our exploration of how climate change affects biodiversity conservation priorities by asking how an MPA network designed for today compares to a network designed for the future. To answer this question, we conducted a biodiversity prioritization with projected species distributions (2050, SRES A2 emissions scenario[11,31]) and seamounts, but excluded biogeographical provinces and current human impacts, because the future spatial configurations of these are presently unknown. The SRES A2 scenario describes a world that is characterized by high regional heterogeneity with continuous population growth in the twenty-first century. Cumulative CO_2 emissions by the middle and end of the twenty-first century are projected to be about 600 and 1,850 Gt C respectively[21]. Data on the future distributions of seabirds were not available, and these species were excluded from these analyses.

National priorities and random analysis

We explored the implications of national planning—whereby priorities are driven by the level of representation of each feature within a country's EEZ—as opposed to globally coordinated planning based on global

feature representation. Effectively, this means running the prioritization independently for each country but with the pixel-specific values (v_{i,j_0}) representing the fraction of the country-level total suitable habitat contained within each pixel. The result is a ranking for each country, which we used to build a global ranking based on the marginal increase in biodiversity benefit arising from each pixel. To measure the implications of this nation-centric approach, we measured the level of protection needed to reach 90% of the total global biodiversity benefits and compared it with the globally coordinated priorities. Finally, we built a null model of biodiversity conservation benefits following a random prioritization by generating 100 sets of randomly ordered pixels and evaluating their performance against a globally optimized solution.

Uncertainty analysis

We assessed the robustness of our results to two common sources of uncertainty in conservation planning: (1) commission errors in species distribution maps; and (2) weighting of individual features. It has been shown that at global and coarse scales, commission errors are more common and important to assess than omission errors as these can introduce an overestimation of biodiversity representation in spatial planning[38,95]. Furthermore, although we aim to minimize the subjectivity of assigning feature weights by using ecologically relevant metrics (extinction risk, evolutionary distinctiveness and functional distinctiveness), these—and our approach to combine them—are only a subset of many possible alternatives. Thus, to investigate these sources of uncertainty we ran 1,000 iterations of the biodiversity prioritization, randomly removing up to 30% of each species distribution, and adding random errors to feature weights in each iteration. The fraction of each species distribution to remove was drawn from a uniform distribution U[0, 0.3], and the errors added to each feature weight (w) were randomly drawn from a uniform distribution U[−sd(w), sd(w)]. We present maps of the fraction of all runs in which each pixel was within the top 5% and 10% of the prioritization solution (Supplementary Figs. 20, 21) as well as a map of the coefficient of variation of each pixel across all runs (Supplementary Fig. 22). Although this approach helps us to assess the robustness of high priority areas for biodiversity conservation, it is limited by the unrealistic assumption that commission errors are randomly distributed. We restrict the assessment of uncertainty to the biodiversity component of our analysis because the carbon, fisheries and human impact components have been assessed elsewhere[29,96].

Reporting summary

Further information on research design is available in the Nature Research Reporting Summary linked to this paper.

Data availability

The underlying data used in this study are available from the sources listed in the Supplementary Information.

Code availability

The R code that supports the findings of this study is available at https://github.com/emlab-ucsb/ocean-conservation-priorities.

47. FAO. *The State of World Fisheries and Aquaculture 2018 – Meeting the Sustainable Development Goals* http://www.fao.org/3/I9540EN/i9540en.pdf (2018).
48. RAM Legacy Stock Assessment Database v.4.44 [Dataset]. https://doi.org/10.5281/zenodo.2542919 (2018).
49. Higgs, N. & Attrill, M. Biases in biodiversity: wide-ranging species are discovered first in the deep sea. *Front. Mar. Sci.* **2**, 61 (2015).
50. Clark, M. R., Watling, L., Rowden, A. A., Guinotte, J. M. & Smith, C. R. A global seamount classification to aid the scientific design of marine protected area networks. *Ocean Coast. Manage.* **54**, 19–36 (2011).
51. Spalding, M. D., Agostini, V. N., Rice, J. & Grant, S. M. Pelagic provinces of the world: a biogeographic classification of the world's surface pelagic waters. *Ocean Coast. Manage.* **60**, 19–30 (2012).
52. Spalding, M. D. et al. Marine ecoregions of the world: a bioregionalization of coastal and shelf areas. *Bioscience* **57**, 573–583 (2007).
53. Watling, L., Guinotte, J., Clark, M. R. & Smith, C. R. A proposed biogeography of the deep ocean floor. *Prog. Oceanogr.* **111**, 91–112 (2013).
54. Thorson, J. T., Munch, S. B., Cope, J. M. & Gao, J. Predicting life history parameters for all fishes worldwide. *Ecol. Appl.* **27**, 2262–2276 (2017).
55. Froese, R. & Pauly, D. FishBase. www.fishbase.org. (2019).
56. Palomares, M. L. D. & Pauly, D. SeaLifeBase. www.sealifebase.org (2019).
57. The Nature Conservancy. Marine Ecoregions and Pelagic Provinces of the World. http://data.unep-wcmc.org/datasets/38 (2012).
58. Halpern, B. S. et al. Recent pace of change in human impact on the world's ocean. *Sci. Rep.* **9**, 11609 (2019).
59. IUCN. 2018 IUCN Red List of Threatened Species. http://www.iucnredlist.org/ (2018).
60. Lehtomäki, J. & Moilanen, A. Methods and workflow for spatial conservation prioritization using zonation. *Environ. Model. Softw.* **47**, 128–137 (2013).
61. Rabosky, D. L. et al. An inverse latitudinal gradient in speciation rate for marine fishes. *Nature* **559**, 392–395 (2018).
62. Stein, R. W. et al. Global priorities for conserving the evolutionary history of sharks, rays and chimaeras. *Nat. Ecol. Evol.* **2**, 288–298 (2018).
63. Fritz, S. A., Bininda-Emonds, O. R. & Purvis, A. Geographical variation in predictors of mammalian extinction risk: big is bad, but only in the tropics. *Ecol. Lett.* **12**, 538–549 (2009).
64. Jetz, W., Thomas, G. H., Joy, J. B., Hartmann, K. & Mooers, A. O. The global diversity of birds in space and time. *Nature* **491**, 444–448 (2012).
65. Violle, C. et al. Functional rarity: the ecology of outliers. *Trends Ecol. Evol.* **32**, 356–367 (2017).
66. May, R. M. Islands biogeography and the design of wildlife preserves. *Nature* **254**, 177–178 (1975).
67. Hubbell, S. P. *The Unified Neutral Theory of Biodiversity and Biogeography (MPB-32)* (Princeton Univ. Press, 2001).
68. Holt, R. D., Lawton, J. H., Polis, G. A. & Martinez, N. D. Trophic rank and the species–area relationship. *Ecology* **80**, 1495–1504 (1999).
69. Tittensor, D. P. et al. Global patterns and predictors of marine biodiversity across taxa. *Nature* **466**, 1098–1101 (2010).
70. Hopf, J. K., Jones, G. P., Williamson, D. H. & Connolly, S. R. Fishery consequences of marine reserves: short-term pain for longer-term gain. *Ecol. Appl.* **26**, 818–829 (2016).
71. Walters, C. J., Hilborn, R. & Parrish, R. An equilibrium model for predicting the efficacy of marine protected areas in coastal environments. *Can. J. Fish. Aquat. Sci.* **64**, 1009–1018 (2007).
72. Guénette, S. & Pitcher, T. J. An age-structured model showing the benefits of marine reserves in controlling overexploitation. *Fish. Res.* **39**, 295–303 (1999).
73. Beverton, R. J. H. & Holt, S. J. *On the Dynamics of Exploited Fish Populations* (Chapman & Hall, 1957).
74. Kroodsma, D. A. et al. Tracking the global footprint of fisheries. *Science* **359**, 904–908 (2018).
75. Eigaard, O. R. et al. Estimating seabed pressure from demersal trawls, seines, and dredges based on gear design and dimensions. *ICES J. Mar. Sci.* **73**, i27–i43 (2016).
76. Hiddink, J. G. et al. Global analysis of depletion and recovery of seabed biota after bottom trawling disturbance. *Proc. Natl Acad. Sci. USA* **114**, 8301–8306 (2017).
77. de Madron, X. D. et al. Trawling-induced resuspension and dispersal of muddy sediments and dissolved elements in the Gulf of Lion (NW Mediterranean). *Cont. Shelf Res.* **25**, 2387–2409 (2005).
78. Ferré, B., De Madron, X. D., Estournel, C., Ulses, C. & Le Corre, G. Impact of natural (waves and currents) and anthropogenic (trawl) resuspension on the export of particulate matter to the open ocean: application to the Gulf of Lion (NW Mediterranean). *Cont. Shelf Res.* **28**, 2071–2091 (2008).
79. Kaiser, M. J., Collie, J. S., Hall, S. J., Jennings, S. & Poiner, I. R. Modification of marine habitats by trawling activities: prognosis and solutions. *Fish Fish.* **3**, 114–136 (2002).
80. Oberle, F. K., Storlazzi, C. D. & Hanebuth, T. J. What a drag: quantifying the global impact of chronic bottom trawling on continental shelf sediment. *J. Mar. Syst.* **159**, 109–119 (2016).
81. Palanques, A., Guillén, J. & Puig, P. Impact of bottom trawling on water turbidity and muddy sediment of an unfished continental shelf. *Limnol. Oceanogr.* **46**, 1100–1110 (2001).
82. Gray, J. in *Oceanography and Marine Biology Annual Review* Vol. 12 (ed. Barnes, H.) 223–261 (George Allen & Unwin, 1974).
83. McArthur, M. et al. On the use of abiotic surrogates to describe marine benthic biodiversity. *Estuar. Coast. Shelf Sci.* **88**, 21–32 (2010).
84. Burdige, D. J. Preservation of organic matter in marine sediments: controls, mechanisms, and an imbalance in sediment organic carbon budgets? *Chem. Rev.* **107**, 467–485 (2007).
85. Spinelli, G. A., Giambalvo, E. R. & Fisher, A. T. in *Hydrogeology of the Oceanic Lithosphere* (eds Davis, E. E. & Elderfield, H.) Ch. 6 (Cambridge Univ. Press, 2004).
86. Arndt, S. et al. Quantifying the degradation of organic matter in marine sediments: a review and synthesis. *Earth Sci. Rev.* **123**, 53–86 (2013).
87. Paraska, D. W., Hipsey, M. R. & Salmon, S. U. Sediment diagenesis models: review of approaches, challenges and opportunities. *Environ. Model. Softw.* **61**, 297–325 (2014).
88. Lovelock, C. E. et al. Assessing the risk of carbon dioxide emissions from blue carbon ecosystems. *Front. Ecol. Environ.* **15**, 257–265 (2017).
89. Wilkinson, G. M., Besterman, A., Buelo, C., Gephart, J. & Pace, M. L. A synthesis of modern organic carbon accumulation rates in coastal and aquatic inland ecosystems. *Sci. Rep.* **8**, 15736 (2018).
90. Rodriguez, A. B., McKee, B. A., Miller, C. B., Bost, M. C. & Atencio, A. N. Coastal sedimentation across North America doubled in the 20th century despite river dams. *Nat. Commun.* **11**, 3249 (2020).
91. Moilanen, A., Leathwick, J. R. & Quinn, J. M. Spatial prioritization of conservation management. *Conserv. Lett.* **4**, 383–393 (2011).

92. Armsworth, P. R. Inclusion of costs in conservation planning depends on limited datasets and hopeful assumptions. *Ann. NY Acad. Sci*. **1322**, 61–76 (2014).
93. Carwardine, J. et al. Conservation planning when costs are uncertain. *Conserv. Biol*. **24**, 1529–1537 (2010).
94. Naidoo, R. et al. Integrating economic costs into conservation planning. *Trends Ecol. Evol*. **21**, 681–687 (2006).
95. Rondinini, C., Wilson, K. A., Boitani, L., Grantham, H. & Possingham, H. P. Tradeoffs of different types of species occurrence data for use in systematic conservation planning. *Ecol. Lett*. **9**, 1136–1145 (2006).
96. Stock, A. & Micheli, F. Effects of model assumptions and data quality on spatial cumulative human impact assessments. *Glob. Ecol. Biogeogr*. **25**, 1321–1332 (2016).

Acknowledgements This study was funded by the National Geographic Society and the Leonardo DiCaprio Foundation. D.M. was supported by the French Foundation for Research on Biodiversity (FRB).

Author contributions E.S., J. Mayorga, D.B., R.B.C., T.B.A., W.C., C.C., F.F., A.M.F., S.D.G., W.G., B.S.H., J. McGowan, D.M., H.P.P., K.D.R., B.W. and J.L. conceived the study and designed the prioritization framework; J. Mayorga, R.B.C., T.B.A., A.A., W.C., A.M.F., C.G., W.G., B.S.H., A.H., K.K., K.K.-R., F.L., L.E.M., D.M., J.P.-A. and B.W. provided data and/or conducted analyses; J. Mayorga, D.B., R.B.C. and A.H. wrote computer code; and E.S., J. Mayorga, D.B., R.B.C., T.B.A., W.C., C.C., F.F., A.M.F., S.D.G., W.G., B.S.H., J. McGowan, L.E.M., D.M., H.P.P., K.D.R., B.W. and J.L. wrote the paper.

Competing interests The authors declare no competing interests.

Additional information

Supplementary information The online version contains supplementary material available at https://doi.org/10.1038/s41586-021-03371-z.

Correspondence and requests for materials should be addressed to E.S.

Peer review information *Nature* thanks Charles Ehler and the other, anonymous, reviewer(s) for their contribution to the peer review of this work.